Changes in Negative Charge at the Luminal Mouth of the Pore Alter Ion Handling and Gating in the Cardiac Ryanodine-Receptor

Fiona C. Mead-Savery,[†] Ruiwu Wang,[‡] Bhavna Tanna-Topan,[†] S. R. Wayne Chen,[‡] William Welch,[§] and Alan J. Williams[†*]

[†]Cardiac Medicine, National Heart and Lung Institute, Faculty of Medicine, Imperial College London, London SW3 6LY, United Kingdom; [‡]Libin Cardiovascular Research Institute of Alberta, Departments of Physiology and Biophysics and of Biochemistry and Molecular Biology, University of Calgary, Calgary, Alberta, Canada; and [§]Department of Biochemistry, University of Nevada School of Medicine, Reno, Nevada

ABSTRACT We have tested the hypothesis that a high density of negative charge at the luminal mouth of the RyR2 pore plays a pivotal role in the high cation conductance and limited selectivity observed in this channel by introducing into each monomer a double point mutation to neutralize acidic residues in this region of the mouse RyR2 channel. The resultant channel, ED4832AA, is capable of functioning as a calcium-release channel in situ. Consistent with our hypothesis, the ED4832AA mutation altered the ion handling characteristics of single RyR2 channels. The mutant channel retains the ability to discriminate between cations and anions but cation conductance is altered significantly. Unitary K^+ conductance is reduced at low levels of activity but increases dramatically as activity is raised and shows little sign of saturation. ED4832AA no longer discriminates between divalent and monovalent cations. In addition, the gating characteristics of single RyR2 channels are altered markedly by residue neutralization. Open probability in the ED4832AA channel is substantially higher than that of the wild-type channel. Moreover, at holding potentials in excess of ± 50 mV several subconductance states become apparent in ED4832AA and are more prevalent at very high holding potentials. These observations are discussed within the structural framework provided by a previously developed model of the RyR2 pore. Our data indicates that neutralization of acidic residues in the luminal mouth of the pore produces wide-ranging changes in the electric field in the pore, the interaction energies of permeant ions in the pore and the stability of the selectivity filter region of the pore, which together contribute to the observed changes ion handling and gating.

INTRODUCTION

The sarcoplasmic reticulum calcium release channel or ryanodine receptor (RyR) is a high-conductance and cation-selective channel, which has unusual characteristics. Although it ideally discriminates between cations and anions, it is relatively nonselective among cations and can conduct both monovalent and divalent cations with a radius of up to ~3.5 Å (1). In addition, it has a very high unitary conductance, reaching a maximum of ~1nS with K^+ as the permeant ion. The structural features of this channel controlling conductance and discrimination are still the subject of speculation, although studies have suggested that, in common with other cation-selective channels, negative charge in the pore may be important (2). Experimental evidence for the existence of negative charge in the conduction pathway of the RyR channel and the involvement of this charge in ion translocation has been provided by monitoring the effects of polycationic blockers (3,4) and charge screening (5,6) on single channel function. In addition, the potential role of negatively charged, electrostatic funnels at the mouths of the RyR pore that might enhance diffusion-limited cation translocation by electrostatic focusing has also been discussed (2,7).

The primary sequence of an important component of the putative pore-forming region of RyR was first identified through the recognition of a GIGD sequence (8,9) as similar to the GYGD selectivity filter motif identified in K^+ channels (10). The importance of this motif, and residues flanking this motif, to RyR channel function was reinforced by data collected from channels containing a variety of point mutations in this region of both RyR1 and RyR2, that showed decreased cation conductance or altered [^{3}H]-ryanodine binding (11–13).

Subsequently, a model of the putative pore-forming region of RyR was constructed using the crystal structure of the KcsA K^+ channel as a template (14). This model contains the GIGD motif in a location equivalent to the selectivity filter of K^+ channels and, in addition, suggests the existence of distinct regions of high negative charge density at both the cytosolic and luminal mouths of the pore. There are two luminal loops with net negative charge; one linking the pore helix and inner helix which forms the central region of the pore and another linking the pore helix with the outer helix. In the RyR2 tetramer these would give rise to an inner and outer ring of acidic residues surrounding the luminal entrance to the pore.

Submitted December 17, 2007, and accepted for publication October 28, 2008.

*Correspondence: williamsaj9@cardiff.ac.uk

Fiona C. Mead-Savery's present address is Heart Science Centre, Laboratory of Cell Electrophysiology, National Heart and Lung Institute, Imperial College London, Harefield Hospital, Harefield, Middlesex UB9 6JH, UK.

Alan J. Williams' present address is Dept. of Cardiology, Wales Heart Research Institute, Cardiff University School of Medicine, Cardiff CF14 4XN, UK.

Editor: David A. Eisner.

0006-3495/09/02/1374/14 $2.00

doi: 10.1016/j.bpj.2008.10.054

Recent information emerging from high resolution cryo-electron microscopy studies of RyR1 is consistent with the proposal that the RyR channel pore is made up of structural elements equivalent to those of K^+ channels (15,16).

Although gross changes brought about by polycation block and charge screening are suggestive of a role for luminal negative charge in ion selection and translocation in RyR, the significance of specific acidic residues in the putative luminal loops is still the subject of investigation. Zorzato et al. (17) have described a central core disease deletion mutation in RyR1 that removes two acidic residues from one of these loops and results in reduced conductance. However, investigations involving the substitution of individual acidic residues that contribute to the inner ring around the luminal mouth of the RyR1 pore have suggested that some of these residues have little functional consequence (11,18). Neutralization in RyR1 of the glutamic acid residue equivalent to E4832 or the aspartic acid residue equivalent to D4833 in RyR2 produced no significant change in K^+ conductance. A similar lack of effect was found after the neutralization of the aspartic acid residue equivalent to D4837 or the glutamic acid residue equivalent to E4840 in RyR2.

The model of wild-type (WT) RyR2 pore (14) contains a total of 48 acidic residues in the loops making up the luminal face of the structure within a solvent accessible surface area of ~7000 $Å^2$. Given the high density of acidic residues in this region of the pore, we reasoned that single neutralizing substitutions may not be sufficient to produce significant changes in the net charge of this region of the pore and hence produce significant changes in the ion handling properties of the channel. As a consequence, in this study we have attempted to reduce the net charge of the luminal mouth of the RyR2 pore by substitution, with alanines, of both E4832 and D4833, a pair of residues in the immediate proximity of the proposed selectivity filter. Whole cell investigations show that the resulting ED4832AA RyR2 is a functional channel that responds to caffeine and ryanodine. However, the gating and ion handling properties of individual ED4832AA channels are significantly different from those of the WT RyR2 channel.

MATERIALS AND METHODS

Site-directed mutagenesis and DNA transfection

Point mutations were introduced into the proposed pore-forming region of the mouse cardiac sarcoplasmic reticulum Ca^{2+}-release channel (RyR2) by the overlapping extension method using polymerase chain reaction as described previously (13). HEK293 cells were grown in Dulbecco's modified Eagle's medium supplemented with 5% fetal bovine serum, 2 mM glutamine and 100 IU/ml penicillin/50μg/ml streptomycin, and were transfected with WT or ED4832AA DNA using the calcium phosphate precipitation method (19).

Ca^{2+} release measurements in transfected HEK293 cells

Free cytosolic Ca^{2+} concentration in transfected HEK293 cells was measured using the fluorescent Ca^{2+} indicator fluo 3-AM as described previously (20) with some modifications. Cells were grown for 18 h after transfection then washed with phosphate-buffered saline containing 137 mM NaCl, 8 mM Na_2HPO_4, 1.5 mM KH_2PO_4 and 2.7 mM KCl. The transfected cells were then shaken gently for 45 min at room temperature in a solution containing 125 mM NaCl, 5 mM KCl, 1.2 mM KH_2PO_4, 6 mM glucose, and 25 mM HEPES (pH 7.4). The cells were harvested, pelleted and resuspended in Dulbecco's modified Eagle's medium and loaded with 10 μM fluo 3-AM for 1 h. The fluo 3-AM loaded cells were washed with KRH buffer (125 mM NaCl, 5 mM KCl, 1.2 mM KH_2PO_4, 6 mM glucose, 1.2 mM $MgCl_2$, 2 mM $CaCl_2$, and 25 mM HEPES (pH 7.4)) then suspended in KRH buffer supplemented with 0.1 mg/ml bovine serum albumen and 250 μM sulphinpyrazone. The fluorescence intensity of fluo 3-AM was monitored at 530 nm both before and after additions of increasing concentrations of caffeine, and after the addition of 2.5 mM caffeine followed by 100 μM ryanodine, with 480 nm excitation at 25°C.

Isolation of expressed channels

HEK293 cells were grown for 24 h after transfection then washed and harvested with phosphate-buffered saline supplemented with 2.5 mM EDTA. Cells were solubilized for an hour on ice in a solution containing 25 mM TRIS, 50 mM HEPES, 137 mM NaCl, 1.0% CHAPS, 0.2% egg phosphatidylcholine, and protease inhibitors. Insoluble material was removed by centrifugation and channel proteins were isolated on a 5–25% continuous sucrose gradient. Fractions containing channel proteins were identified using [^{3}H]-ryanodine binding. Channel protein-containing fractions were aliquoted, snap frozen and stored in liquid nitrogen.

Single channel recording

Individual channels were incorporated into phosphatidylethanolamine (Avanti Polar Lipids, Alabaster, AL) planar bilayers as described previously (21). To investigate effects of varying K^+ activity, bilayers were initially formed in symmetrical solutions of 100 mM, 210 mM, 410 mM, 610 mM, or 1 M KCl with 20 mM HEPES, pH 7.4. Isolated channels were added to the *cis* chamber and incorporation into the bilayer was stimulated by the addition of aliquots of 3 M KCl to the *cis* chamber to form an osmotic gradient. RyR2 incorporates into the bilayer in a fixed orientation in such a way that the *cis* chamber corresponds to the cytosolic face of the channel and the *trans* chamber corresponds to the luminal face (21). The *cis* chamber was perfused with the appropriate solution after single channel incorporation. K^+ activities were calculated using appropriate activity coefficients taken from Hamer and Wu as quoted in (22). For investigations involving Ba^{2+}, bilayers were formed initially in symmetrical 210 mM KCl. An indication of the affinity of channels for Ba^{2+} was obtained by adding increasing concentrations of the cation to the *trans* chamber as a permeant blocker of K^+ translocation.

The permeability of ions relative to K^+ was determined by monitoring reversal potentials after the creation of the appropriate ionic gradient. With 210 mM KCl in the *cis* chamber the relative permeabilities of K^+ and Cl^- were determined by perfusion of the *trans* chamber with 810 mM KCl. To determine the relative permeability of the channel to K^+ and Ba^{2+} the *trans* chamber was perfused with 210 mM $BaCl_2$ adjusted to pH 7.4 with 40 mM HEPES. Junction potentials were determined as described (23) and measured reversal potentials corrected accordingly.

The contaminating free-Ca^{2+} concentration of solutions was monitored using a calcium-sensitive electrode as described previously (24) and found to be ~10 μM. Experiments were performed at room temperature (21 ± 2°C).

Data acquisition and analysis

Single channel current fluctuations were low-pass filtered with an 8-pole Bessel filter at either 1 or 5 kHz and sampled at 20 kHz with a PCI-6036E AD board (National Instruments, Austin, TX) for acquisition using Acquire 5.0.1 (Bruxton, Seattle, WA). Single channel current amplitudes were measured directly on screen using Review 5.0.1 or from all-point histograms using TACx4.1.5 (Bruxton).

Theoretical modeling and molecular dynamics simulations

The construction of the WT and ED4832AA RyR2 pore models and molecular dynamics simulations within these models were carried out as described previously (14). To probe the environment of a permeant ion in the pore, explicit solvation (TIP3 water) was used. Weak distance and torsion constraints were applied to the helices to replace the stabilizing forces provided by the transmembrane helices omitted from the models of the RyR pore. The constraints prevent long term drifting of the positions of the helices. The forces were adjusted to provide a < 2 Å rms deviation of the backbone atoms of the helices regardless of the length of the molecular dynamics simulation. Unless stated otherwise, the loops and selectivity filter of the pore lacked imposed constraints. Potassium and chloride ions were added to simulate changes in ionic strength. Except for simulations at "zero" ionic strength, the ensemble was electrically neutral.

We have investigated the consequences of the ED4832AA substitution by monitoring two parameters in the WT and ED4832AA model pores; the electric field and the interaction energy of a single permeant potassium ion. Although these parameters are related, the relationship is complex. We define the electric field as the global (macroscopic) property described by Coulomb's law. When using the term electric field we assume a continuum dielectric in both the protein and water components of the system. The change in electric field is visualized by using the Poisson-Boltzmann approximation. In these calculations the dielectric constant of solvent was set to 78, the dielectric constant of the protein was set to 4 and the Stern layer was set to the average radius of the K^+ and Cl^- ions (1.57 Å).

We define the interaction energy as the microscopic interaction of a permeant ion with the surroundings including water, protein and counter-ions. In a molecular mechanics force field these will be simulated by the nonbonded interactions (Coulomb and Lennard-Jones interactions). Outside the pore, the calculated energy of interaction is similar to the standard state enthalpy of hydration ($K^+ = -85$ kcal/mol (25)).

AMBER7–9 and SYBYL 7.1–8.0 were used for the computational studies.

Materials

Phosphatidylethanolamine was obtained from Avanti Polar Lipids. Cell culture materials were obtained from Invitrogen (Paisley, UK). [^{3}H]-ryanodine was obtained from Amersham Biosciences (Little Chalfont, Bucks, UK). All other materials were obtained from VWR (Poole, UK) or Sigma-Aldrich (Poole, UK).

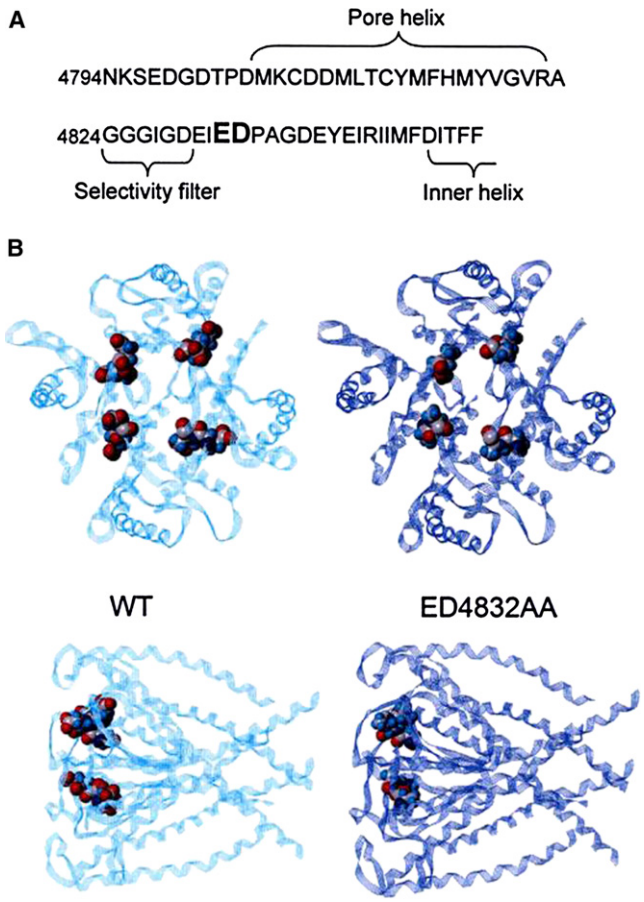

FIGURE 1 (*A*) Amino acid sequence of a portion of the pore-forming region of the mouse RyR2 channel. E4832 and D4833 (highlighted in bold) are in close proximity to the series of residues equivalent to the selectivity filter in K^+ channels. (*B*) Pore models of WT and ED4832AA RyR2 channel tetramers. The luminal faces of the models are shown in the upper panels and side views of the models are shown in the lower panels. In both cases the bulk of the structure is shown as ribbons with E4832 and D4833 in the WT and A4832 and A4833 in ED4832AA in CPK.

RESULTS

Selection of residues for investigation and consequences of residue substitution

The locations of E4832 and D4833 within the primary sequence of RyR2 and within the pore model are shown in Fig. 1. Fig. 1 *B* shows views from the luminal face and side of models of both the WT pore and the pore in which E4832 and D4833 have been replaced by alanine residues. Neutralization of the two acidic residues in each monomer does not produce major disruption within the pore model. The stability of the wild-type tetramer and ED4832AA can be compared using a pseudo energy function (a function based on the probability of finding a particular residue in a particular three-dimensional environment). Both WT and ED4832AA have a global pseudo energy equal to +0.02 kT (for comparison, the 1BL8 Protein Data Bank structure of KcsA has a pseudo energy equal to +0.05 kT). More precisely, the residue 4832 region has highly favorable pseudo energy (14). The replacement of E4832 and D4833 by alanines adds +0.02 kT to the pseudo energy of this region.

Effect of the ED4832AA substitutions on the in situ response of RyR2 to caffeine and ryanodine

We characterized the functional state of the ED4832AA RyR2 channel in intact HEK cells by using a Ca^{2+} release assay in which RyR-mediated release was monitored using the fluorescent indicator fluo 3-AM. Caffeine-induced Ca^{2+} release was monitored in intact HEK cells expressing the ED4832AA channel over a range of concentrations from 0.025 mM to 5 mM and after addition of 100 μM ryanodine. Responses are shown in Fig. 2. The cells responded in a manner similar to HEK cells expressing the WT channel

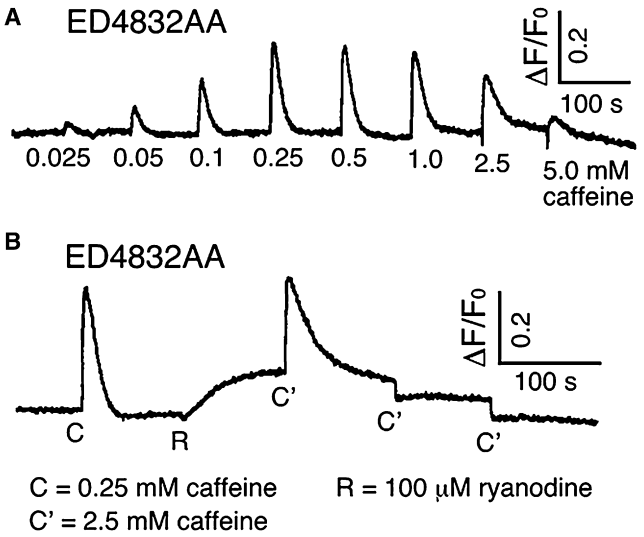

FIGURE 2 Effects of caffeine (*A*) and caffeine and ryanodine (*B*) on Ca^{2+} release from intracellular stores in HEK cells transfected with the ED4832AA mutant. Fluorescence of Fluo-3 AM loaded cells was monitored continuously before and after addition of increasing concentrations of caffeine, or 0.25 mM caffeine (denoted *C*), 100 μM ryanodine and 2.5 mM caffeine (denoted *C'*). Traces shown are from a representative experiment that has been repeated three times. Similar responses were measured in all three experiments.

(26,27) indicating that the ED4832AA RyR2 forms a functional channel capable of releasing Ca^{2+} in response to caffeine and ryanodine. As noted in earlier studies with cells expressing the WT channel, the amplitude of Ca^{2+}-release events in cells expressing ED4832AA decreases at caffeine concentrations in excess of 1.0 mM; presumably as the result of depletion of intracellular stores (26,27).

Single channel observations

Our in situ studies have established that the ED4832AA RyR2 functions as a Ca^{2+}-release channel; however, to assess the impact of the double neutralizing substitution on the mechanisms underlying ion translocation and discrimination, it is necessary to characterize the function of single voltage-clamped channels under a wide range of ionic conditions.

After reconstitution into planar phospholipid bilayers in symmetrical 210 mM KCl and with μM cytosolic Ca^{2+} as the sole activating ligand, WT RyR2 characteristically fluctuated between a single open and a single closed state. In comparison, under these experimental conditions ED4832AA channels had a reduced unitary conductance (see subsequent sections) and a markedly higher open probability (Po). At holding potentials of $< \pm$ 50 mV closing events of ED4832AA occurred rarely and were very brief. At higher holding potentials, although full closing events remained rare, a wide range of well resolved subconductance states were observed. Fig. 3 shows representative traces of WT (Fig. 3 *A*) and ED4832AA (Fig. 3 *B*) RyR2 channels at a holding potential of +90 mV, together with the associated

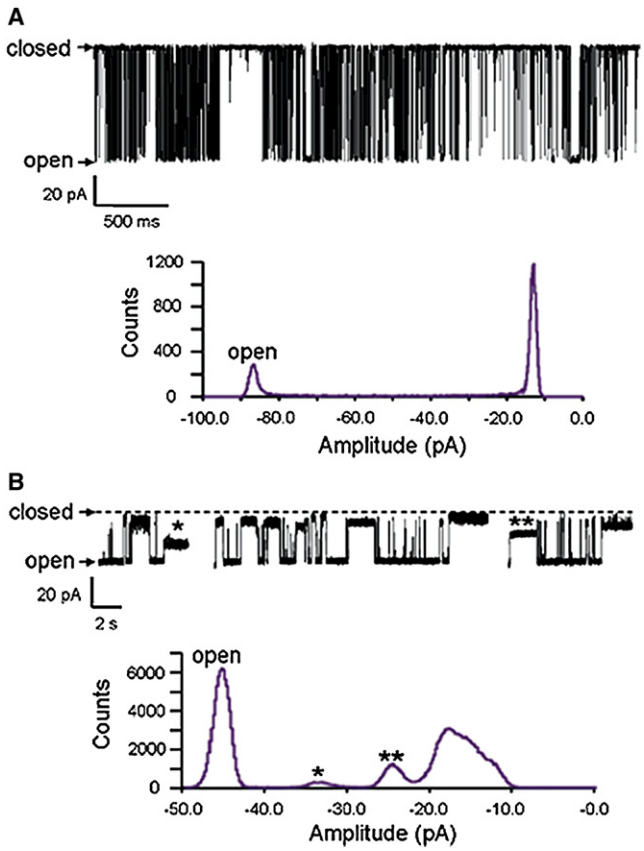

FIGURE 3 Single channel current fluctuations of individual WT and ED4832AA RyR2 channels in symmetric 210 mM KCl at a holding potential of +90 mV. Under these conditions the WT channel alternates between a single open and a single closed state (*A*). In contrast the ED4832AA channel spends lengthy periods in a range of subconductance states. *B* shows three representative sections of data from a single ED4832AA RyR2 channel together with a cumulative amplitude histogram collected for this channel over a total recording time of 78 s. The representative traces demonstrate the very wide range of subconductance states that characterize the ED4832AA RyR2 channel. The vast majority of these events have amplitudes of <50% of the full open state. Indeed the amplitudes of the bulk of these events are so similar that they appear as a smeared peak to the right of the associated amplitude histogram. Only two subconductance states (indicated by *asterisks* in the traces and histogram of *B*) can be resolved with any degree of confidence.

amplitude histograms. Although single open and closed states were resolved in the WT channel, many, relatively long lasting subconductance states were seen in ED4832AA. The bulk of these events have amplitudes of <50% of the full open state. The very great similarity in the amplitude of the majority of the events makes an assessment of the probability of their occurrence and the distribution of the lifetimes of the individual events extremely difficult and this has not been attempted in this study.

At holding potentials in excess of $\pm$ 80 mV the ED4832AA channel can reside for long periods in a subconductance state of very low conductance (not shown). In these cases the channel will reopen after reversal of the holding potential.

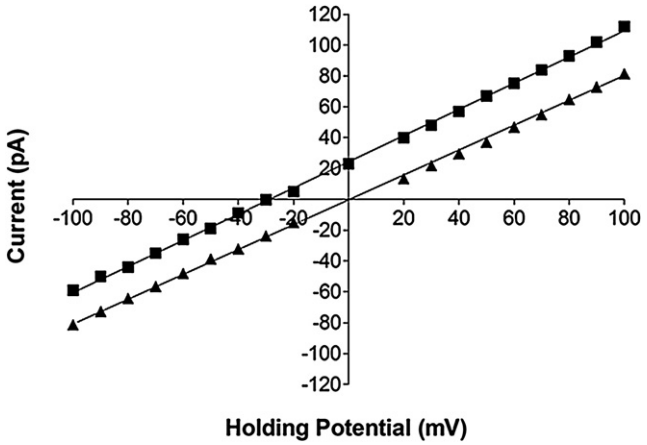

FIGURE 4 Cation-anion discrimination in the ED4832AA mutant. Current-voltage plots showing single channel current amplitude in the ED4832AA mutant in symmetric 210 mM KCl (▲) and asymmetric KCl (210 mM trans; 810 mM *cis*) (■). The linear regression line plotted through the asymmetric K^+ data indicates a reversal potential of −30 mV and demonstrates that the channel retains the ability to discriminate between cations and anions. All points are mean values ± SE derived from four or more experiments. Error bars are within the symbol.

Is the ED4832 RyR2 channel cation-selective?

Measurements of ED4832AA functioning in intact cells and at the single channel level have demonstrated that the ED4832AA channel is permeable to both divalent and monovalent cations. As an initial step in the characterization of ion handling, we have determined if the ED4832AA channel retains the ability to discriminate between cations and anions. Current amplitudes were measured over a range of holding potentials from −100 to 100 mV in asymmetric conditions with 210 mM KCl, 20 mM HEPES in the *trans* chamber or luminal side of the channel and 810 mM KCl, 20 mM HEPES in the *cis* chamber or cytosolic side of the channel. The resultant plot of unitary current against holding potential shows a linear relationship (Fig. 4), with a reversal potential of −30 mV. This compares favorably with a predicted value of −34 mV calculated from the Nernst equation for a channel that is ideally selective for K^+ over Cl^-:

$$E_K = \frac{RT}{zF} \times \ln \frac{[K^+]_{trans}}{[K^+]_{cis}}. \quad (1)$$

These experiments demonstrate that the neutralization of a total of eight negatively charged luminal residues (two in each monomer) in close proximity to the proposed selectivity filter has not brought about a marked change in the ability of RyR2 to discriminate between cations and anions.

Altered potassium conductance properties in the ED4832AA RyR2 channel

The aim of this study was to consider the ion handling properties of a RyR2 channel with a reduced net negative charge at the luminal mouth of the conduction pathway. As a starting point K^+ conductance was examined in individual ED4832AA channels and compared with conductance measured in the WT channel.

K^+ conductance was assessed by monitoring the relationship between unitary current and holding potential in symmetrical KCl solutions of increasing concentration. Representative traces for both WT and ED4832AA channels are shown in Fig. 5. The resulting current-voltage plots are presented in Fig. 6. The graph in Fig. 6 *A* shows the response of the WT channel to varying holding potentials monitored in 210 mM and 610 mM KCl. It is apparent from this graph that there is little change in the slope of the relationship plotted from data generated in the two K^+ solutions tested. The slope conductance calculated for the WT channel in 210 mM KCl is 806 ± 4 pS, which increases to a value of 887 ± 3 pS in 610 mM KCl. This observation is consistent

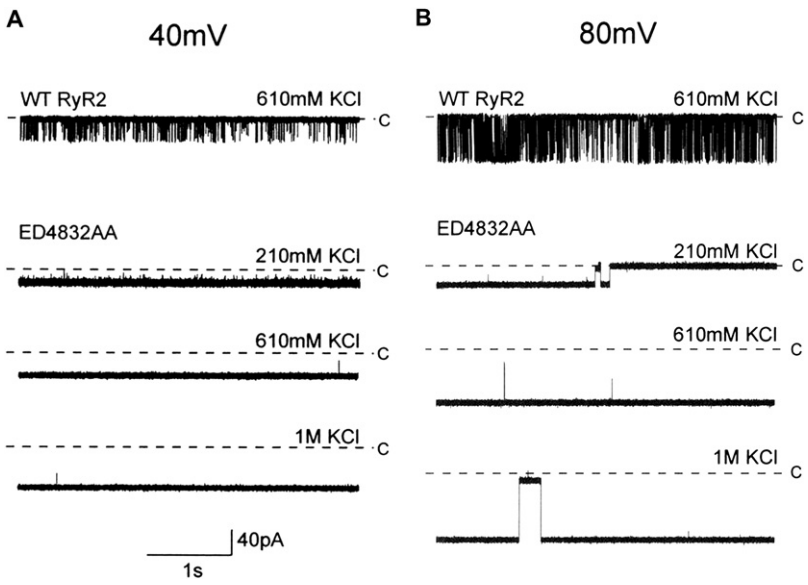

FIGURE 5 Single channel traces showing increased P_o and altered conductance of the ED4832AA mutant at a range of ionic activities. (*A*) At 40 mV, P_o compared to WT is extremely high, as shown by openings as downward deflections with very few closings. (*B*) At 80 mV, openings are long, but subconductance states are apparent. Closed level denoted by *C*.

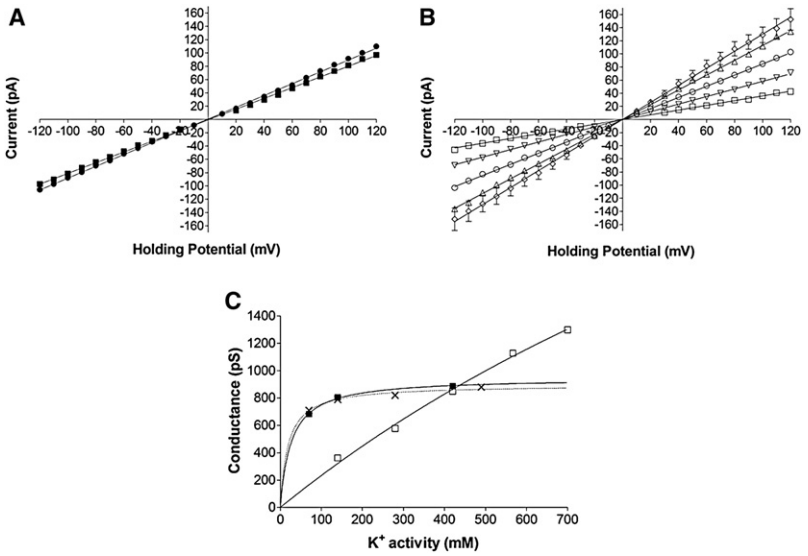

FIGURE 6 (*A*) Current-voltage plot for the mouse WT channel in symmetrical K^+ solutions. Slope conductance measured in 210 mM KCl (■) was 806 ± 4 pS compared to 887 ± 3 pS measured in 610 mM KCl (●). (*B*) Current-voltage relationships ED4832AA in symmetrical 210 mM (□), 410 mM (▽), 610 mM (○), 810 mM (△), and 1 M (◇) KCl. In both *A* and *B*, solid lines are derived from linear regression. All points are mean values ± SE derived from four or more experiments. Error bars, where not visible, are within the symbol. The graph in *C* demonstrates the change in RyR2 slope conductance in response to increasing K^+ activity. ED4832AA (□); recombinant mouse WT (■) and native RyR2 isolated from sheep cardiac muscle (X). Lines are nonlinear regression derived from a single site binding hyperbola. All points are mean values ± SE derived from four or more experiments. Error bars are within the symbol.

with data obtained previously using WT RyR2 channels isolated from sheep cardiac muscle in which a slope conductance of 723 ± 9 pS was measured in symmetrical 210 mM KCl and a saturating maximum conductance of 900 pS was determined as K^+ activity was increased (28).

The relationship between slope conductance and K^+ activity is altered dramatically by the neutralization of the eight acidic luminal residues. The plot in Fig. 6 *B* shows the relationship between current and holding potential for ED4832AA channels in symmetrical KCl solutions ranging from 210 mM to 1 M. In 210 mM KCl the slope conductance measured in the ED4832AA channel is significantly lower than that measured in the WT channel. The value calculated using linear regression is 362 ± 3 pS compared to 806 ± 4 pS in WT. However, as K^+ concentration increases to 610 mM, the slope conductance rises to 850 ± 2 pS, a value very similar to the slope conductance for the WT channel in 610 mM KCl. When the concentration of the permeant ion is increased still further to 810 mM and 1 M, the slope conductance of ED4832AA continues to increase and eventually exceeds 1000 pS.

All slope conductance values calculated using linear regression from the data shown in Fig. 6, *A* and *B* have been plotted against K^+ activity in Fig. 6 *C*. Data obtained previously with sheep WT RyR2 channels (28) have been included for comparison. As can be seen from the graph, the slope conductance of the mouse WT RyR2 channel expressed in HEK cells, in common with the isolated WT sheep RyR2, saturates at K^+ activities above 200 mM. The K^+ activity at which 50% saturation is observed in the mouse WT channel is 26.4 ± 2.5 mM.

Neutralization of E4832 and D4833 produces a profound alteration in K^+-handling in RyR2. At activities below 400 mM neutralization results in a reduced rate of translocation. At activities in excess of 400 mM rates of K^+ translocation are markedly greater than those seen in the WT channel. The ED4832AA channel exhibits little sign of saturation with K^+ activities within the range tested, and, as a consequence, it is not possible to determine an activity at which 50% saturation occurs.

Relative permeability of monovalent and divalent cations in WT and ED4832AA channels

The investigations reported in this communication thus far have established that a reduction in negative charge at the luminal entrance of the RyR2 pore a), has little or no effect upon the ability of RyR2 to discriminate between monovalent cations and anions and b), results in markedly different, activity-dependent, rates of K^+ translocation with little indication of saturation at high K^+ activities. To gain a more complete understanding of the mechanisms governing ion translocation and discrimination in the ED4832AA RyR2 channel, and hence the mechanisms underlying function of the WT RyR2 channel, we have monitored the relative ability of the two channels to discriminate between monovalent and divalent cations.

Previous studies have shown that although RyR2 is a relatively nonselective cation channel, it can discriminate between divalent and monovalent cations. In sheep WT RyR2, the relative permeabilities of alkaline earth divalent cations have been calculated under bi-ionic conditions against K^+ to give pX^{2+}/pK^+ values of ~6.5 (2). In this study, Ba^{2+} was chosen as a representative divalent ion rather than Ca^{2+} (the physiologically relevant alkaline earth divalent) to prevent complications caused by the varied gating effects that can result from changes in either cytosolic or luminal Ca^{2+} concentrations. Current fluctuations of either WT or ED4832AA channels were monitored with 210 mM KCl *cis*, and 210 mM $BaCl_2$ *trans*. The resulting current-voltage relationships are presented in Fig. 7.

In agreement with our earlier investigations with WT sheep RyR2 channels, the WT mouse RyR2 expressed in HEK cells is more permeable to Ba^{2+} than K^+. Under the

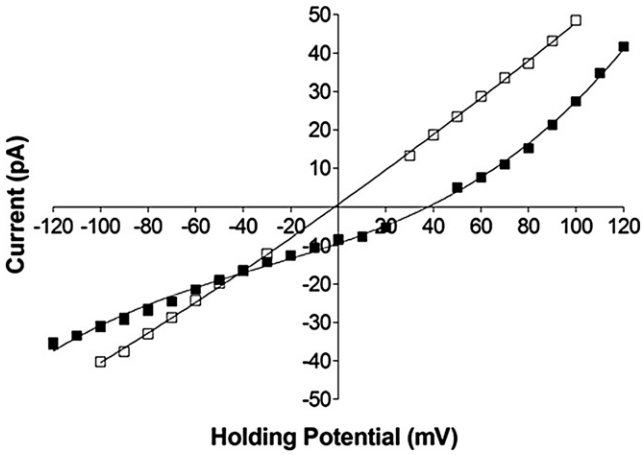

FIGURE 7 Current-voltage plots showing the altered response of ED4832AA (□) compared to WT mouse RyR2 (■) in asymmetric conditions of 210 mM KCl (*cis*) and 210 mM $BaCl_2$ (*trans*). The reversal potential determined for the WT mouse channel is 38 mV and that of ED4832AA is 0 mV. Solid lines have no mathematical significance. All points are mean values ± SE derived from four or more experiments. Error bars, where not visible, are within the symbol.

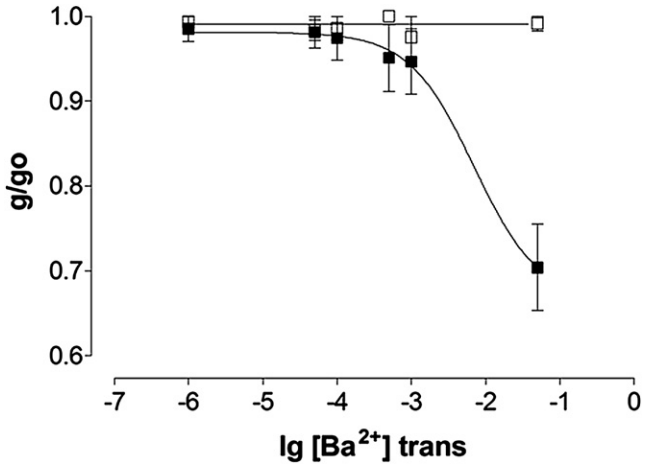

FIGURE 8 Ba^{2+} block of K^+ current in WT (■) and ED4832AA (□) RyR2 channels. Unitary conductance at −60 mV (expressed as a proportion of conductance at 60 mV) plotted against Ba^{2+} concentration at the luminal (*trans*) side of the channel. All points are mean values ± SE derived from four or more experiments. Solid lines have no mathematical significance.

conditions used in these experiments, unitary current reverses at a holding potential of 38 mV. The permeability of Ba^{2+} relative to K^+ can then be calculated using the relationship derived by Fatt and Ginsborg (29),

$$\frac{P_{Ba^{2+}}}{P_{K^+}} = \frac{[K^+]}{[Ba^{2+}]} \times \frac{\exp(E_{rev}F/RT)[\exp(E_{rev}F/RT) + 1]}{4}, \quad (2)$$

yielding a value of pBa^{2+}/pK^+ of 6.3 in the WT mouse channel.

A reduction in the negative charge at the luminal entrance of the RyR2 pore after the neutralization of E4832 and D4833 results in a very significant alteration of the relative permeability of divalent and monovalent cations in the RyR2 channel. Under the conditions used in these experiments, unitary current in the ED4832AA channel reverses at a holding potential of 0 mV, indicating that the channel displays no discernable discrimination between Ba^{2+} and K^+.

In addition to information on the relative permeability of ions, experiments such as those shown in Fig. 7 can also provide information on the conductance of the ions under investigation. Under the conditions used in these experiments, at extreme positive holding potentials the channels will be carrying essentially pure K^+ current and at extreme negative holding potentials, essentially pure Ba^{2+} current. As a result the slopes of the relationships at these extremes yield measurements of slope conductance equivalent to those obtained under symmetrical ionic conditions (23). An examination of the slopes of the relationships at and above +80 mV demonstrate that, as was noted in Fig. 6, in the presence of 210 mM K^+ the conductance of the ED4832AA channel is lower than that of the WT channel. In contrast, an examination of the slopes of the relationships at and lower than − 80 mV indicates that the conductance of the ED4832AA channel with 210 mM Ba^{2+} as the charge carrier is greater than that of the WT channel. As a consequence of these changes, although in the WT channel slope conductance for 210 mM K^+ is 3.6 times greater than the equivalent value in 210 mM Ba^{2+}, in ED4832AA the slope conductance for 210 mM K^+ is merely 1.2 times greater than the equivalent value in 210 mM Ba^{2+}.

Ba^{2+} block of K^+ translocation in WT and ED4832AA RyR2 channels

The data presented in Figs. 6 and 7 indicate that a reduction in the negative charge at the luminal entrance of the mouse RyR2 pore, resulting from the neutralization of E4832 and D4833, brings about a very significant alteration in the interaction of monovalent and divalent cations with the channel pore. Our previous investigations with the sheep WT channel have established that the affinity of the channel for divalent cations is ~140 times greater than that for monovalents; assessed by using Ba^{2+} as a permeant blocker of K^+ current (2).

We have carried out a similar series of experiments with the WT and ED4832AA mouse RyR2 channels. Channel function was monitored in symmetrical 210 mM KCl with increasing concentrations of $BaCl_2$ added to the solution at the luminal side of the channel. Current amplitude was measured at ±60 mV and the relative conductance at −60 mV (expressed as a proportion of conductance at +60 mV) is plotted against Ba^{2+} concentration in Fig. 8.

As is the case for the WT sheep RyR2 channel, increasing concentrations of luminal Ba^{2+} block K^+ current in WT mouse channels. Block is discernable at Ba^{2+} concentrations of 100 μM and above and relative conductance is reduced by 30% in the presence of 50 mM Ba^{2+}. In contrast, there is no

observable reduction in relative conductance at any luminal Ba^{2+} concentration up to 50 mM in the ED4832AA channel. These experiments demonstrate that neutralization of negative charge at the luminal entrance of the RyR2 pore drastically reduces the strength of interaction of divalent cations with the channel pore. The complete absence of block by 50 mM Ba^{2+} in the presence of 210 mM K^+ indicates that the strength of interaction of Ba^{2+} and K^+ with ED4832AA channel pore is likely to be comparable.

Simulations in the WT and ED4832AA RyR2 pore models: a comparison of the electric field, interaction energy and selectivity filter stability

Fig. 9 illustrates how the ED4832AA substitution alters the distribution of electric field at the solvent accessible surface of the protein. Only the pore region of the RyR is modeled; therefore we show views of the pore from the lumen (Fig. 9, *top four panels*) and the cytosol (Fig. 9, *bottom four panels*). At zero ionic strength the mutation produces a large decrease in negative electric field at the surface of the luminal loops (compare left and right panels in Fig. 9, *row A*) but much less change at the cytosolic entrance (compare left and right panels in Fig. 9, *row C*). Because of the differential ability of mutant and WT to concentrate counter ions, high ionic strength largely masks the difference at the two entrances of the channels (Fig. 9, *rows B* and *D*). In contrast, ionic strength produces much less change in electric field at the surfaces deep within the pore (compare the color in the center of each panel at 0 and 500 mM ionic strength; for example, *rows A* and *B* in the RyR2 column of Fig. 9). This is a result of microenvironmental effects arising from the limited access of ions and water to the pore (for example, the selectivity filter). Changes in electric field at the selectivity filter will be described more quantitatively below.

In earlier investigations we performed a series of simulations of ion translocation in the WT RyR2 pore model. These studies demonstrated that experimental parameters of ion translocation and block in RyR2 could be qualitatively simulated in the model and identified major sites of interaction between permeant and impermeant ions and amino acid residues in the pore region of the channel (14). In Fig. 10 we present a comparative simulation of ion translocation in the WT and ED4832AA RyR2 pore models. The system is simulated in explicit water at zero ionic strength. Zero ionic strength is chosen to reveal the intrinsic differences in the pores of the WT and mutant RyR2 pores. A single K^+ is undergoing biased diffusion through the pores of the two RyR models and the figure shows the change in interaction energy as the ion moves from the lumen (0 Å), through the pore, before emerging in the cytosol (100 Å). The simulation in the WT channel reveals a deep interaction energy minimum centered approximately in the middle of the selectivity filter (*A*: 40 Å) with a maximum as the ion leaves the

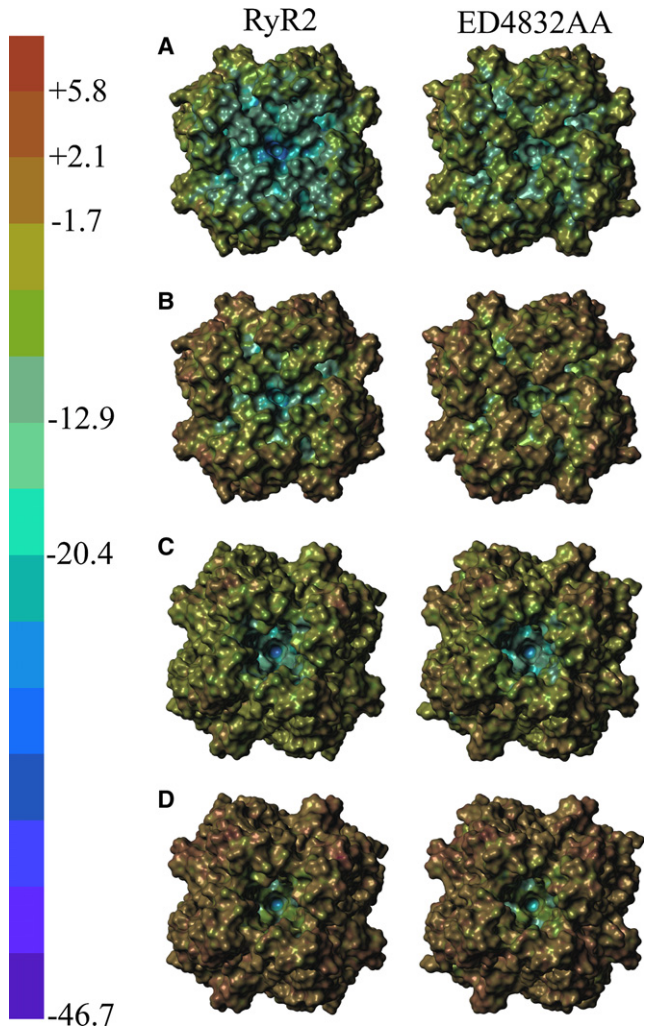

FIGURE 9 Poisson-Boltzmann electric field. The electric field at the solvent accessible surface of the RyR2 pore model was calculated by the Poisson-Boltzmann equation and visualized by the color scale on the left. The left column contains WT RyR2 and the right column contains the ED4832AA mutant. The top four panels (*rows A* and *B*) view the pore region from the lumen; the bottom four panels (*rows C* and *D*) view the pore from the cytosol. The electric field is computed at 0 (*rows A* and *C*) and 500 mM (*rows B* and *D*) ionic strength (KCl).

selectivity filter and moves into the central vestibule of the pore (*B*: 53–54 Å). The second deep minimum is in the putative gate region at the crossover of the inner helices (*C*: 71 Å). Note that when the K^+ emerges into the cytosol, as expected, the energy of the ion returns to the level that it had before entering the channel from the lumen.

In these simulations the permeant ion does not simply interact with a gradient of electric field such as illustrated in Fig. 9, but rather with a collection of ionic groups from the protein (e.g., glutamate residues), other ions in solution (e.g., potassium, chloride), moving electric dipoles from the protein (e.g., the peptide carbonyl groups) and the reorienting dipoles from water. These factors will be affected by the electric field. In molecular mechanics, interactions

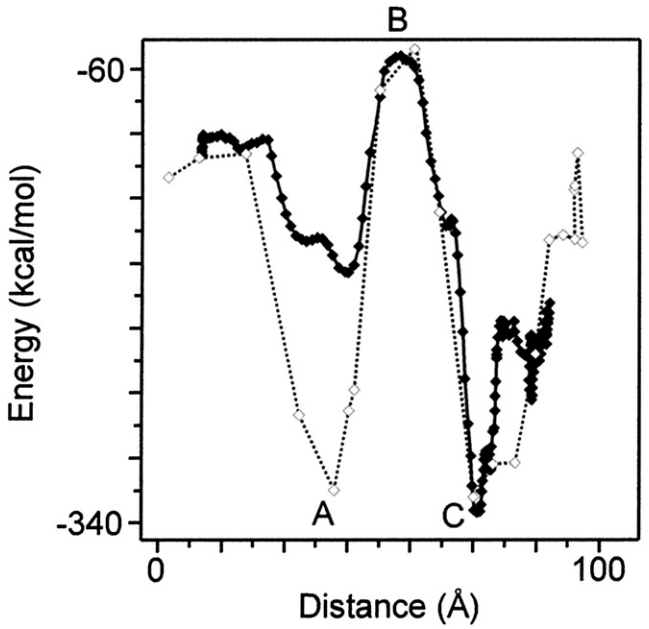

FIGURE 10 Molecular dynamics simulations in the WT and ED4832AA mouse RyR2 model pores. A comparison of the energy of interaction of a single K^+ ion as it moves from the solution at the luminal side of the pore (0 Å), through the pore, and emerges in the cytosol (100 Å) (WT (◇) ED4832AA (◆)). Explicit solvation (TIP3 water) was used in this simulation. No counter ions were included: thus, these simulations are effectively at zero ionic strength. Please note that the energy scale is that of AMBER7 and is for comparison only. As a reference point, the standard state enthalpy of hydration of K^+ is −85 kcal/mol. The figure shows the effect of both the change in the number of ionic groups and the conformational changes induced by the double mutation. First minimum (*A*: 39 Å) is at the level of Ile-4827 within the selectivity filter. The large maximum (*B*: 53–54 Å) is in the middle of the cytosolic vestibule at the imaginary apex of the pore helices. The nearest amino acid residue (Ile-4867, TM4) is 5–6 Å distant. The next minimum (*C*: 71 Å) is at the level of Asp-4875/Gln-4879 (TM4). The ion is between these two residues at this distance.

between the permeant ion and the surroundings are estimated from Coulombs Law and the Lennard-Jones potential.

Fig. 10 illustrates how the presence of the protein perturbs the interaction between the permeant potassium ion and the atoms surrounding it. Outside of the pore, the interaction energy is approximately that of the experimental enthalpy of hydration of the potassium ion. The RyR2 structure strongly perturbs this quantity. The strongest excursions are found in the regions of the selectivity filter and the putative gate. Mutation to ED4832AA has the most profound effect in the selectivity filter. To compare Figs. 9 and 10, we have estimated the electric field in Fig. 9 at the 40 Å mark (the minimum in interaction energy in Fig. 10). A numerical solution to the Poisson-Boltzmann method was used. At zero ionic strength, WT RyR2 has a value of −35 kcal/mol; the ED4832AA substitution lowers the value to −28 kcal/mol. Increasing ionic strength to 500 mM (with KCl) decreases the WT value from −35 kcal/mol to −29 kcal/mol; increasing ionic strength lowers the ED3842AA value from -28 kcal/mol to −22 kcal/mol. To compare the effect of the double mutation at zero ionic strength we estimate that the mutation lowers the electric field to 80% of that of the WT (−28 mut vs. −35 wt). In contrast, the mutation lowers the interaction energy to 48% of that of the WT. Therefore, electric field and interaction energy do not directly correlate. This point will be explored in more detail below.

Molecular dynamics simulations in the WT and ED4832AA RyR2 models also reveal differences in the stability of the selectivity filter region of the structures. In the WT pore the side chain of Glu-4832 maintains strong interactions with the side chains of Tyr-4839, Arg-4843 and Thr-4849 on adjacent chains. The side chain of Asp-4833 maintains strong interactions with the side chains of Asn-4794 and Lys-4795 on adjacent chains. The combination of ionic and hydrogen bonds between adjacent chains helps stabilize the selectivity filter. These multiple reinforcing interactions are lost in the ED4832AA double mutant. We monitored the consequences of the ED4832AA substitution by measuring the radius of gyration of the selectivity filter (taken as the backbone atoms of Gly-4824 through Asp-4829) and the radius of gyration of Gly-4826 at either low (10 mM KCl) or high (500 mM KCl) ionic strength. The radius of gyration of the selectivity filter of the WT pore was 9.3 ± 0.2 Å (10 mM KCl) and 9.1 ± 0.2 Å (500 mM KCl). The corresponding values for ED4832AA are 7.0 ± 0.1 Å and 10.1 ± 0.2 Å. The radii of gyration of Gly-4826 of WT are 8.5 ± 0.3 Å (10 mM KCl) and 8.3 ± 0.3 Å (500 mM KCl). The corresponding values for ED4832AA are 3.8 ± 0.2 Å (10 mM KCl) and 8.9 ± 0.3 Å (500 mM KCl). These simulations demonstrate that the selectivity filter of the WT pore has little sensitivity to K^+ concentration whereas the selectivity filter of the ED4832AA pore expands as K^+ concentration increases.

In the following section, we present a series of simulations to demonstrate how the interaction energies of a probe K^+ ion with its surroundings will be affected by changes in its environment.

Group 1 simulations

In the first example, a single potassium ion is tethered to the 40 Å position (Fig. 10, location *A*, the interaction energy minimum in the selectivity filter) whereas the motions of protein, water, and counter ions are not explicitly restricted. The pores of both WT RyR2 and ED4832AA were packed with potassium and chloride ions and the systems brought to thermal equilibrium. Under these unnatural conditions the selectivity region is disoriented (denatured) and the probe K^+ ion is surrounded with potassium and chloride ions. RyR2 had an interaction energy = −222 ± 83 kcal/mol (or slightly more than one standard deviation of the value in the absence of any supporting counter ions, Fig. 10) whereas interaction energy of ED4832AA = −330 ± 33 kcal/mol. This

simulation serves as a control or baseline. When the probe K^+ ion is surrounded by a cloud of potassium and chloride ions, the interaction energy is high and strongly shielded from the change in the electric field resulting from the mutated residues. In other words, the impossibly excessive packing of KCl almost abolished the difference between WT and ED4832AA substituted RyR2 pores. This is not unexpected as the interactions of the neighboring potassium and chloride ions make more of a contribution to the interaction energy of the probe K^+ ion than the distant carboxyl groups.

Group 2 simulations

In the next group of simulations, potassium and chloride ions were placed around the model of RyR2 pore (to make the system electrically neutral) and the system solvated and equilibrated to 300 K. The resulting systems contain 0.4–0.5 M potassium ions. To view the effect of charge only (and eliminating the accompanying conformational changes), in these simulations the positions of the permeant ion and the backbone of the protein are fixed whereas the motions of side chains, water, and counter ions are not explicitly restricted. The probe K^+ ion is again at the 40 Å position (location *A* in Fig. 10). These simulations differ from the Group 1 simulations in that the potassium and chloride ions are largely at the ends of the channel and few ions are within the pore. The interaction energy of RyR2 was -399 ± 31 kcal/mol. The WT RyR2 was then mutated to ED4832AA. The interaction energy of ED4832AA $= -333 \pm 33$ kcal/mol. Unlike the example above, protein (not a cloud of KCl) intervenes between the probe K^+ ion and the mutated amino acids. Comparing these interaction energies to those at the equivalent position (*A*: 40 Å) at zero ionic strength in Fig. 10, increasing the ionic strength had little effect on the interaction energy of RyR2. Freezing ED4832AA in one of the RyR2 conformers prevents the decrease in interaction energy observed when the selectivity filter is allowed to undergo the mutation-induced conformational change.

Group 3 simulations

The Group 2 simulations were continued after removing the restriction on the movement of the protein backbone. Earlier we described the effect of the ED4832AA substitution on the physical stability of the selectivity filter. Here we investigate the effect on interaction energy. As above, the probe K^+ ion is restrained to the 40 Å position. In the case of the WT channel, the interaction energy remains ~ -320 kcal/mol regardless of ionic strength ($[K^+] = 0$ M; -333 ± 27 kcal/mol, $[K^+] = 0.48$ M; -323 ± 33 kcal/mol). In contrast, the interaction energy of ED4832AA begins decreasing immediately after release of the restraint on the protein and equilibrates at ~ -170 kcal/mol ($[K^+] = 0$ M; -160 ± 37 kcal/mol, $[K^+] = 0.49$ M; -169 ± 57 kcal/mol). Again, ionic strength has little effect on the interaction energy. As highlighted above, the ED4832AA substitution allows greater motional freedom to the selectivity filter than is found in the WT RyR2 pore. It appears that mutation-induced conformational changes in the selectivity filter have a greater impact on interaction energy than mutation-induced changes in electric field.

Group 4 simulations

In analogous simulations to those described in Group 2 above, a probe K^+ ion was allowed free diffusion at the luminal entrance of RyR2. As above, the peptide backbone of the channel was immobilized. This group of simulations differs from group 2 simulations because the probe K^+ ion has been removed from the restricted confines of the selectivity filter to the face of the pore where it faces the full onslaught of the counter ions. As in group 2 simulations, the backbone atoms of the protein are fixed. In general, ionic strength decreases electric field by increasing the effective dielectric constant. Ionic strength does not weaken ionic interactions by altering the intrinsic affinity for binding: ligands are released by increased competition for binding sites (for example, as observed in ion exchange chromatography). Interactions of the probe K^+ ion were explored at the highest and lowest interaction energies observed in the simulations. A 3 Å radius was used to define these close contacts. These residues are on the loop between the selectivity filter and TM4 (the transmembrane helix lining the cytosolic cavity of the pore model (14)). At the highest (-285 kcal/mol) interaction energy, the K^+ ion interacts with the aromatic ring of Tyr-4839, one water, a strong interaction with the side chain carboxyl of Glu-4832 (van der Waals contact) and a weaker interaction with the carboxylate side chain of Glu-4840 (a 5 Å distance). All residues are on the same subunit. At the lowest interaction energy (-444 kcal/mol) the potassium ion interacts with four waters, and the peptide oxygens of residues Glu-4832 and Asp-4833 (both on the same subunit). Because of thermal motion at 300 K the potassium can move rapidly. In this case, the K^+ moved from lowest energy to highest energy in 4 ps (5.5 Å). The WT channel was mutated to ED4832AA and the simulation repeated. At the lowest interaction energy (-339 kcal/mol) the K^+ ion interacts with three water molecules, the peptide oxygen of residue Asp-4829 and water bridged to the side chain carboxyl of Glu-4830. At the highest (-243 kcal/mol) interaction energy, the K^+ ion interacts with the side chain carboxylate of Glu-4830, and one water molecule. One of the waters had diffused away (but was still within 3.5 Å) and the other was now more than 3.5 Å away. The overlapping ranges indicate that even when the ion is located outside of the pore, the loss of electric field is significant but does not eradicate the large changes in interaction energy resulting from the close order (microscopic, explicit) interactions between ion and protein.

In summary, the foregoing simulations have highlighted the following likely consequences of the ED4832AA substitution in the RyR2 pore: a), substitution of E4832 and D4833 with alanines produces major changes in the electric field both at the luminal face of the RyR2 pore and in the electric field of the selectivity filter of the pore at low ionic strength b), increasing ionic strength masks the substitution-induced difference in electric field at the luminal face of the pore but not that in the selectivity filter. From this we infer that WT and ED4832AA differ in their ability to concentrate ions at the entrance of the pore and (at least in WT) that the microenvironment of the selectivity filter largely insulates this region from changes in the bulk solvent. c), the double substitution causes the loss of up to eight salt links that stabilize the conformation of the selectivity filter in the WT pore. d), increasing ionic strength causes conformational changes in the selectivity filter of ED4832AA, but not the WT channel. e), the substitution perturbs the strength of interaction between permeant ions and their surroundings primarily at the selectivity filter.

We suggest that all of these factors will contribute to the alterations in RyR2 ion handling and gating reported in this communication.

DISCUSSION

Our model of the RyR channel pore (14) indicates that both the luminal and cytosolic mouths of the RyR2 pore contain high densities of acidic residues giving rise to significant negative charge in both of these regions of the channel and we have hypothesized that these closely packed acidic residues may provide mechanisms for maximizing rates of cation delivery to the pore, for discrimination between anions and cations and for the observed limited discrimination between divalent and monovalent cations (14). In our study, we have used recombinant WT and mutant mouse RyR2 together with the measurement of whole cell Ca^{2+} transients, single channel ion handling and molecular modeling to investigate the potential role of acidic residues, localized in the luminal mouth of the RyR2 channel, in channel function.

Our results demonstrate that the neutralization, in each monomer, of a pair of luminal acidic residues, E4832 and D4833, by mutation to alanine yields a RyR2 channel that functions as a regulated Ca^{2+}-release channel when expressed in HEK cells. However analysis of the properties of individual channels reveals that residue neutralization has very significant consequences for channel function. The most obvious effect of the substitution is a dramatic increase in the P_o of the channel compared to WT and the occurrence of well defined subconductance states at high holding potentials (Fig. 3). Comparing the ion-handling properties of ED4832AA with the WT channel we find that neutralization does not alter the ability of RyR2 to discriminate between monovalent cations and anions (Fig. 4) but does result in a very significant modification of unitary K^+ conductance (Figs. 5 and 6). The magnitude of the change in unitary conductance is dependent upon K^+ activity and we observe little or no indication of saturation (Fig. 6). Neutralization of E4832 and D4833 also abolishes the ability of RyR2 to discriminate between divalent (Ba^{2+}) and monovalent (K^+) cations (Fig. 7), produces an increase in Ba^{2+} conductance (Fig. 7) and abolishes the ability of Ba^{2+} to act as a permeant blocker of K^+ translocation (Fig. 8).

Mechanisms underlying the observed changes in cation conductance

It is well established that surface charge in both the intracellular and extracellular mouths of plasma membrane ion channels plays a significant role in ion conduction (30–36), ion discrimination (37,38) and block (33,39). The influence of charged residues in the mouths of ion channels on rates of ion translocation is generally accepted to be mediated by modulation of the rate of entry of ions into the pore. Rings of acidic residues in the mouths of K^+ channels produce negative electrostatic potentials which facilitate the accumulation of K^+ and raise the activity of the permeant ion above that of the bulk solution. Neutralization of these residues, either by chemical modification (30) or by residue substitution (33) results in reductions in unitary conductance and an apparent lowering of the affinity of the pore for the translocated ion. Important characteristics of this mechanism are that the reduction of unitary conductance is most marked at low ion activities and that, although charge neutralization takes place on only one side of the pore, both extracellular to cytosolic and cytosolic to extracellular currents are reduced symmetrically (30). As permeant ion activity is increased the influence of reduced charge diminishes, so that conductance approaches control values at saturating activities where rates of ion entry are no longer rate limiting.

Data derived from the calculation of the electric fields at the solvent accessible surface of the pore and molecular dynamic simulations in the WT and ED4832AA models demonstrate that the neutralization of acidic residues results in a small but significant reduction in the electric field at the luminal face of the pore at low ionic strength and this is likely to contribute to the reduced conductance of ED4832AA observed at the lower K^+ activities. However, it is clear that the neutralization of E4832 and D4833 does more than simply change the effective concentration of permeant cations at the luminal entrance of the RyR2 pore. The increase in unitary conductance of both K^+ and Ba^{2+} in ED4832AA, above the saturating values monitored in WT RyR2, demonstrates that additional mechanisms are involved.

In the experimental protocol used in these experiments, potassium ions are principally translocated through the WT RyR2 by the applied transmembrane potential. The relationship between current and applied potential is linear from 0 to 120 mV (see Fig. 6 *A*) without a hint of approach to another rate limiting step. However, if transport through the pore

were entirely electrophoretic, the current would be proportional to the product of the concentration (of K^+) and force (applied potential). This is not the case for RyR2. The WT RyR2 current is essentially independent of K^+ concentration above 100 mM.

Experimentally, RyR2 behaves as an enzyme with Michaelis-Menten kinetics. A K^+ ion forms a Michaelis complex, is translocated across the pore, forms a second Michaelis complex, and is then released into the bulk solvent on the opposite side of the membrane. At concentrations >100 mM, the RyR2 is saturated with K^+ at all applied potentials and the translocation step is always rate limiting. Under these conditions the Michaelis-Menten equation $v = V_{max}$ [K]/(K_M + [K]) becomes $v = V_{max} \cong 90$ pA (at 100 mV) (Fig. 6 *A*).

However, transport across the ED4832AA mutant is qualitatively different. The current is directly proportional to the product of concentration and applied potential at all conditions measured. Using the enzyme model above, one explanation is that the mutation increased the Michaelis constant to >10 M. In this limit, the Michaelis-Menten equation becomes $v = (V_{max}/K_M)$ [K]. However, if this were true, the predicted current would differ from the experimentally measured current. For example, at 100 mV and 210 mM K^+ the predicted current is ~2 pA compared to the observed 30 pA. Similar arguments based on altering V_{max} also fail the arithmetic test.

Alternatively, one might view the difference in ion transport of WT and ED4832AA in terms of conductance. In the case of WT RyR2, increases in K^+ concentration above a certain level do not change the conductance of RyR2. In other words, the channel conductance does not increase proportionally to the conductance of the bulk solvent. The geometry of the pore (selectivity filter) restricts access of ions and water: the microenvironment insulates the pore from changes in bulk solvent. We suggest that the mutation causes an alteration of the selectivity filter such that its conductance is no longer isolated from that of the bulk solution and varies proportionally with K^+ concentration. This model is consistent with the experimental observation that, for ED4832AA, current is proportional to the product of applied potential and K^+ concentration. We suggest that the large qualitative difference in conductance between WT and ED4832AA has its origin in the major difference in electric field in the selectivity filter and the differences in the conformational dynamics of the residues comprising the selectivity filter identified in the comparison of the WT and ED4832AA pore models. In terms of enzymology, the mutations have reorganized the active site, making WT and ED4832AA qualitatively different enzymes.

Mechanisms underlying the observed loss of discrimination between divalent and monovalent cations

In addition to the alteration in conductance discussed above, neutralization of E4832 and D4833 induces a profound change in the ability of the RyR2 channel to discriminate between divalent and monovalent cations. Although the WT channel displays a limited preference for divalent cations, ED4832AA is equally permeable to Ba^{2+} and K^+.

In K^+ channels a very high degree of discrimination between cations is achieved as the result of interactions with a series of backbone carbonyl oxygens of highly conserved residues making up the selectivity filter (10,40). Given the much lower degree of discrimination displayed by RyR2, it is unlikely that an equivalent mechanism is employed in this channel. We have previously proposed that the limited selectivity found in RyR could be achieved if the channel possessed a high density of negative charge either within the pore or within vestibules at either end of the pore (2). Results in this communication indicate that a reduction in charge density at the luminal mouth of the pore could contribute to the loss of cation discrimination seen in ED4832AA. Possibly of more significance are the large changes in the electric field and the loss of stabilizing interactions within the selectivity filter that result from the neutralization of these residues.

Although E4832 and D4833 are essential for discrimination between divalent and monovalent cations, they are not required for discrimination between cations and anions in RyR2 (Fig. 4). Neutralization of rings of charged residues in the 5-HT_3 receptor has been shown to abolish discrimination between anions and cations in this channel (37) and it is probable that acidic residues located elsewhere within the luminal mouth of RyR2 (14) contribute to the discrimination between cations and anions.

Mechanisms underlying altered gating and the occurrence of subconductance states in ED4832AA

The hypothesis that we set out to test in these investigations was that a ring of negatively charged residues in the luminal mouth of RyR2 played a significant role in regulating ion translocation and discrimination in this channel. An unexpected finding of our experiments was that neutralization of E4832 and D4833 resulted in a very significant change in the gating properties of the RyR2 channel. In the presence of μM cytosolic Ca^{2+} as the only activating ligand, the P_o of ED4832AA channels was invariably dramatically higher than WT channels under the same conditions. In addition ED4832AA channels displayed several well defined subconductance states, the probability of the occurrence of which was increased as the holding potential was raised.

Increased P_o

Mutation of residues in the selectivity filters and extracellular mouths of various K^+ channels (equivalent to the luminal mouth of RyR2) produce alterations in gating ((41) and citations therein). Interestingly, it has recently been demonstrated

that interactions involving a glutamic acid residue in the proximity of the signature selectivity sequence of KcsA contribute to the destabilization of the conductive conformation of the selectivity filter in this channel. Neutralization of E71 by mutation to alanine prevents this destabilizing interaction and results in greatly increased P_o (42).

Our observation that stabilizing interactions in the selectivity filter region of the WT RyR2 pore are lost in the ED4832AA channel raises the possibility that these interactions are involved in the stabilization of a closed conformation of the WT pore and that loss of these interactions underlies the observed dramatic increase in P_o.

Occurrence of subconductance states in ED4832AA at high holding potentials

Well resolved subconductance states are a feature of many species of ion channel and their occurrence can depend upon a wide range of mechanisms (43). One of the mechanisms discussed by Dani and Fox (43) is particularly relevant to this report. They demonstrated that in channels with large mouths containing net negative charge, subconductance states can arise from small conformational changes that alter the electric field or affect the ability of this region of the channel to bind ions. Clearly RyR2 falls into this category of ion channel; why then do we only see well resolved subconductance states after the neutralization of E4832 and D4833?

A likely explanation comes from the reduced stability of the selectivity filter of the pore of ED4832AA highlighted in previous sections of this communication. Reduced stability in this region of the channel may well result in conformational changes such as those described by Dani and Fox (43). The likelihood of conformational change could be enhanced as the applied potential across the channel is increased, accounting for the higher probability of occurrence of subconductance states at high holding potentials. A related mechanism has been proposed to account for the occurrence of subconductance states in Kir2.1 (35).

In summary, the data presented in this communication indicate that neutralization of a pair of acidic residues localized close to the luminal entrance of the selectivity filter in each monomer of the RyR2 channel changes both ion handling and gating properties of the channel. Information obtained from a comparison of models of the two pores indicates that neutralization of E4832 and D4833 is likely to result, as expected, in a decrease in cation binding in the luminal mouth of the channel at low ionic strength. In addition, residue substitution produces a very significant reduction in the interaction energy between a permeant cation and the selectivity filter of the channel and destabilization of this region of the pore. All of these mechanisms are likely to contribute to the alterations in RyR2 channel function observed in this study.

The authors thank Jeff Bolstad and Jennifer Weismann for excellent technical assistance.

This work was supported by grants from the British Heart Foundation (RG/03/003) to A.J.W.; National Science Foundation Molecular and Cellular Biosciences 9817605 to W.W., and the Canadian Institutes of Health Research and the Heart and Stroke Foundation of Alberta, Northwest Territories, and Nunavut to S.R.W.C.

REFERENCES

1. Tinker, A., and A. J. Williams. 1993. Probing the structure of the conduction pathway of the sheep cardiac sarcoplasmic reticulum calcium-release channel with permeant and impermeant organic cations. *J. Gen. Physiol.* 102:1107–1129.
2. Tinker, A., A. R. G. Lindsay, and A. J. Williams. 1992. A model for ionic conduction in the ryanodine receptor-channel of sheep cardiac muscle sarcoplasmic reticulum. *J. Gen. Physiol.* 100:495–517.
3. Mead, F. C., D. Sullivan, and A. J. Williams. 1998. Evidence for negative charge in the conduction pathway of the cardiac ryanodine receptor channel provided by the interaction of K^+ channel N-type inactivation peptides. *J. Membr. Biol.* 163:225–234.
4. Mead, F. C., and A. J. Williams. 2002. Block of the ryanodine receptor channel by neomycin is relieved at high holding potentials. *Biophys. J.* 82:1953–1963.
5. Mead, F. C., and A. J. Williams. 2004. Electrostatic mechanisms underlie neomycin block of the cardiac ryanodine receptor channel (RyR2). *Biophys. J.* 87:3814–3825.
6. Tu, Q., P. Velez, M. Cortes-Gutierrez, and M. Fill. 1994. Surface charge potentiates conduction through the cardiac ryanodine receptor channel. *J. Gen. Physiol.* 103:853–867.
7. Mejía-Alvarez, R., C. Kettlun, E. Ríos, M. Stern, and M. Fill. 1999. Unitary Ca^{2+} current through cardiac ryanodine receptor channels under quasi-physiological ionic conditions. *J. Gen. Physiol.* 113: 177–186.
8. Balshaw, D., L. Gao, and G. Meissner. 1999. Luminal loop of the ryanodine receptor: A pore-forming segment? *Proc. Natl. Acad. Sci. USA.* 96:3345–3347.
9. Zhao, M. C., P. Li, X. L. Li, L. Zhang, R. J. Winkfein, et al. 1999. Molecular identification of the ryanodine receptor pore-forming segment. *J. Biol. Chem.* 274:25971–25974.
10. Doyle, D. A., J. M. Cabral, R. A. Pfuetzner, A. L. Kuo, J. M. Gulbis, et al. 1998. The structure of the potassium channel: Molecular basis of K^+ conduction and selectivity. *Science.* 280:69–77.
11. Gao, L., D. Balshaw, L. Xu, A. Tripathy, C. L. Xin, and G. Meissner. 2000. Evidence for a role of the lumenal M3–M4 loop in skeletal muscle Ca^{2+} release channel (ryanodine receptor) activity and conductance. *Biophys. J.* 79:828–840.
12. Du, G. G., X. H. Guo, V. K. Khanna, and D. H. MacLennan. 2001. Functional characterization of mutants in the predicted pore region of the rabbit cardiac muscle Ca^{2+} release channel (Ryanodine receptor isoform 2). *J. Biol. Chem.* 276:31760–31771.
13. Chen, S. R. W., P. Li, M. C. Zhao, X. L. Li, and L. Zhang. 2002. Role of the proposed pore-forming segment of the Ca^{2+} release channel (ryanodine receptor) in ryanodine interaction. *Biophys. J.* 82:2436–2447.
14. Welch, W., S. Rheault, D. J. West, and A. J. Williams. 2004. A model of the putative pore region of the cardiac ryanodine receptor channel. *Biophys. J.* 87:2335–2351.
15. Samsó, M., T. Wagenknecht, and P. D. Allen. 2005. Internal structure and visualization of transmembrane domains of the RyR1 calcium release channel by cryo-EM. *Nat. Struct. Mol. Biol.* 12:539–544.
16. Ludtke, S. J., I. I. Serysheva, S. L. Hamilton, and W. Chiu. 2005. The pore structure of the closed RyR1 channel. *Structure.* 13:1203–1211.
17. Zorzato, F., N. Yamaguchi, L. Xu, G. Meissner, C. R. Muller, et al. 2003. Clinical and functional effects of a deletion in a COOH-terminal lumenal loop of the skeletal muscle ryanodine receptor. *Hum. Mol. Genet.* 12:379–388.
18. Wang, Y., L. Xu, D. A. Pasek, D. Gillespie, and G. Meissner. 2005. Probing the role of negatively charged amino acid residues in ion

permeation of skeletal muscle ryanodine receptor. *Biophys. J.* 89:256–265.

19. Sambrook, J., E. F. Fritsch, and T. Maniatis. 1989. Molecular Cloning. A Laboratory Manual. Cold Spring Harbor Laboratory Press, New York.
20. Li, P., and S. R. W. Chen. 2001. Molecular basis of Ca^{2+} activation of the mouse cardiac Ca^{2+} release channel (ryanodine receptor). *J. Gen. Physiol.* 118:33–44.
21. Sitsapesan, R., and A. J. Williams. 1994. Gating of the native and purified cardiac SR Ca^{2+}-release channel with monovalent cations as permeant species. *Biophys. J.* 67:1484–1494.
22. Lobo, V. M. M. 1989. Handbook of Electrolyte Solutions. Elsevier, Amsterdam.
23. Tinker, A., and A. J. Williams. 1992. Divalent cation conduction in the ryanodine receptor-channel of sheep cardiac muscle sarcoplasmic reticulum. *J. Gen. Physiol.* 100:479–493.
24. Sitsapesan, R., and A. J. Williams. 1994. Regulation of the gating of the sheep cardiac sarcoplasmic reticulum Ca^{2+}-release channel by luminal Ca^{2+}. *J. Membr. Biol.* 137:215–226.
25. Hille, B. 1992. Ionic channels of Excitable Membranes. Sinauer Associates, Sunderland, MA.
26. Wang, R., L. Zhang, J. Bolstad, N. Diao, C. Brown, et al. 2003. Residue Gln4863 within a predicted transmembrane sequence of the Ca^{2+} release channel (ryanodine receptor) is critical for ryanodine interaction. *J. Biol. Chem.* 278:51557–51565.
27. Wang, R., J. Bolstad, H. Kong, L. Zhang, C. Brown, et al. 2004. The predicted TM10 transmembrane sequence of the cardiac Ca^{2+} release channel (ryanodine receptor) is crucial for channel activation and gating. *J. Biol. Chem.* 279:3635–3642.
28. Lindsay, A. R. G., S. D. Manning, and A. J. Williams. 1991. Monovalent cation conductance in the ryanodine receptor-channel of sheep cardiac muscle sarcoplasmic reticulum. *J. Physiol.* 439:463–480.
29. Fatt, P., and B. L. Ginsborg. 1958. The ionic requirements for the production of action potentials in crustacean muscle fibres. *J. Physiol.* 142:516–543.
30. MacKinnon, R., R. Latorre, and C. Miller. 1989. Role of surface electrostatics in the operation of a high- conductance Ca^{2+}-activated K^+ channel. *Biochemistry.* 28:8092–8099.
31. MacKinnon, R., and C. Miller. 1989. Functional modification of a Ca^{2+}-activated K^+ channel by trimethyloxonium. *Biochemistry.* 28:8087–8092.
32. Nimigean, C. M., J. S. Chappie, and C. Miller. 2003. Electrostatic tuning of ion conductance in potassium channels. *Biochemistry.* 42:9263–9268.
33. Haug, T., D. Sigg, S. Ciani, L. Toro, E. Stefani, et al. 2004. Regulation of K^+ flow by a ring of negative charges in the outer pore of BKCa channels. Part I: Aspartate 292 modulates K^+ conduction by external surface charge effect. *J. Gen. Physiol.* 124:173–184.
34. D'Avanzo, N., H. C. Cho, I. Tolokh, R. Pekhletski, I. Tolokh, et al. 2005. Conduction through the inward rectifier potassium channel, Kir2.1, is increased by negatively charged extracellular residues. *J. Gen. Physiol.* 125:493–503.
35. Chang, H. K., S. H. Yeh, and R. C. Shieh. 2005. A ring of negative charges in the intracellular vestibule of Kir2.1 channel modulates K^+ permeation. *Biophys. J.* 88:243–254.
36. Aubin, C. N. S., and P. Linsdell. 2006. Positive charges at the intracellular mouth of the pore regulate anion conduction in the CFTR chloride channel. *J. Gen. Physiol.* 128:535–545.
37. Thompson, A. J., and S. C. R. Lummis. 2003. A single ring of charged amino acids at one end of the pore can control ion selectivity in the 5–HT3 receptor. *Br. J. Pharmacol.* 140:359–365.
38. Bichet, D., M. Grabe, Y. N. Jan, and L. Y. Jan. 2006. Electrostatic interactions in the channel cavity as an important determinant of potassium channel selectivity. *Proc. Natl. Acad. Sci. USA.* 103:14355–14360.
39. Zhang, Y., X. Niu, T. I. Brelidze, and K. L. Magleby. 2006. Ring of negative charge in BK channels facilitates block by intracellular Mg^{2+} and polyamines through electrostatics. *J. Gen. Physiol.* 128:185–202.
40. Noskov, S. Y., and B. Roux. 2006. Ion selectivity in potassium channels. *Biophys. Chem.* 124:279–291.
41. Proks, P., C. E. Capener, P. Jones, and F. M. Ashcroft. 2001. Mutations within the P-loop of Kir6.2 Modulate the intraburst kinetics of the ATP-sensitive potassium channel. *J. Gen. Physiol.* 118:341–353.
42. Cordero-Morales, J. F., L. G. Cuello, Y. Zhao, V. Jogini, D. M. Cortes, et al. 2006. Molecular determinants of gating at the potassium-channel selectivity filter. *Nat. Struct. Mol. Biol.* 13:311–318.
43. Dani, J. A., and J. A. Fox. 1991. Examination of subconductance levels arising from a single ion channel. *J. Theor. Biol.* 153:401–423.